Carbon fluxes in spring wheat agroecosystems in India

K. N. Reddy[1*], S. Gahlot[1], S. Baidya Roy[1], V. K. Sehgal[2], and V. Gayatri[1]

[1] Centre for Atmospheric Sciences, Indian Institute of Technology Delhi, New Delhi, India.

[2] Division of Agricultural Physics, ICAR-Indian Agricultural Research Institute, New Delhi, India.

Corresponding author: K Narender Reddy (knreddy@cas.iitd.ac.in)

Key Points:

- Carbon fluxes in spring wheat agroecosystems vary widely across India due to divergent climatic conditions and management practices, primarily due to different planting dates.
- All carbon fluxes showed an increasing trend during the 1980 to 2016 study period.
- Providing sufficient fertilizers and water through irrigation may be able to counteract the adverse effects of high temperatures on carbon fluxes.

Abstract

Carbon fluxes from agroecosystems contribute to the variability in the carbon cycle and atmospheric [CO_2]. In this study, we used the Integrated Science Assessment Model (ISAM) equipped with a spring wheat module to study carbon fluxes and their variability in spring wheat agroecosystems of India. First, ISAM was run in the site-scale mode to simulate the Gross Primary Production (GPP), Total Ecosystem Respiration (TER), and Net Ecosystem Production (NEP) over an experimental spring wheat site in the north India. Comparison with flux-tower observations showed that the spring wheat module in ISAM can match the observed flux patterns better than generic crop models. Next, regional-scale runs were conducted to simulate carbon fluxes across the country for the 1980-2016 period. Results showed that the fluxes vary widely, primarily due to variations in planting dates across regions. Fluxes peak earlier in the eastern and central parts of the country, where the crops are planted earlier. All fluxes show statistically significant increasing trends ($p<.01$) during the study period. The GPP, Net Primary Production (NPP), Autotrophic respiration (Ra), and Heterotrophic Respiration (Rh) increased at 1.272, 0.945, 0.579, 0.328, and 0.366 TgC/yr^2, respectively. Numerical experiments were conducted to study how natural forcings like changing temperature and [CO_2] and agricultural management practices like nitrogen fertilization and water availability could contribute to the increasing trends. The experiments revealed that increasing [CO2], nitrogen fertilization, and water added through irrigation contributed to the increase of carbon fluxes, with nitrogen fertilization having the strongest effect.

1 Introduction

Croplands are highly productive ecosystems that interact with the atmosphere by exchanging energy, carbon, and water (Lokupitiya et al., 2016). Croplands take up a large amount of carbon from the atmosphere during their short growing season and contribute to the seasonal-scale variability in atmospheric carbon loading. The increase in the atmosphere's carbon levels has complex impacts on agricultural productivity (Yoshimoto et al., 2005; Saha et al., 2020). Temperature, nitrogen fertilizers, and irrigation are all factors that affect crop development and therefore alter the carbon fluxes from the croplands (Lin et al., 2021). Increased temperature can counteract the beneficial effects of increased carbon in the atmosphere (Sonkar et al., 2019). Better-fertilized soils can react better to higher carbon levels (Lin et al., 2021). Lands with limited

water availability result in reduced carbon fluxes (Hatfield and Prueger, 2015; Green et al., 2019). Hence, understanding the variability and drivers of carbon fluxes from agroecosystems can help better understand the interactions between the biosphere and atmosphere.

Wheat is one of the most widely farmed cereal crops globally and one of the most important staple foods for approximately 2.5 billion people worldwide (Ramadas et al., 2020). Two cultural types of wheat are grown worldwide: winter wheat and spring wheat. Winter wheat is grown in areas with cold weather across Europe, Australia, Russia, and the USA, where it undergoes vernalization during the winter season. Spring wheat is grown in tropical and sub-tropical regions during winters where the temperatures are warmer. In India, spring wheat is generally sown in October-November and harvested between March and April (Ramadas et al., 2020). Spring wheat is the second-largest crop in India in terms of production and cultivated area after paddy. India is second to China in wheat production, with about 107 Mt in 2020, contributing 13.5% of the global wheat supply (FAOSTAT, 2019). Wheat production in India has been on the rise, increasing by 25% since 2008. The area harvested has risen from 28 Mha in 2008 to 29 Mha in 2019 (FAOSTAT, 2019) making spring wheat the second-largest agroecosystem in the country. However, studies of carbon in spring wheat croplands are limited. An extensive review of the variability of carbon fluxes from terrestrial ecosystems conducted by Baldocchi et al. (2018) lacks studies from Indian subcontinent. Hence, this paper focuses on carbon dynamics and its drivers in spring wheat agroecosystems of India.

Although many studies have explored carbon fluxes in various terrestrial ecosystems (Zeng et al., 2020), studies on Indian agroecosystems are limited. Most studies in India estimating carbon fluxes have focused on forest biomes (Jha et al., 2013; Pillai et al., 2019). Jha et al. were the first to discuss carbon and energy fluxes across forest biomes. The authors propose that more flux towers be installed in various vegetation ecosystems to generate a robust carbon flux database (Jha et al., 2013). Pillai et al. (2019) investigated the seasonal variation of NEE in the forest biome using flux tower data and a process-based model (Pillai et al., 2019). The research on forest biomes revealed information about India's forest ecosystems that act as carbon sinks. However, agroecosystems are different from the forest biomes not only because the species composition is different but also because agroecosystems are extensively managed. Human intervention in croplands occur through

fertilization, pest control activities, tillering, irrigation, and harvesting. Therefore, it is essential to understand the impact of the human management practices on carbon fluxes in agroecosystems.

A few studies have looked at carbon fluxes at the site scale over spring wheat agroecosystems in northern India. These include Patel et al. (2011) for the 2008-2009 growing season, Patel et al. (2021) for the 2014-15 growing season, and Kumar et al. (2021) for the 2013-14 growing season. All studies found the typical U-shaped curve in the NEP at diurnal and seasonal scales. The average growing season NEP was in the 5-6 $gC/m^2/d^1$. Patel et al (2021) also reported a negative correlation of NEP with temperature due to higher respiratory losses at higher temperatures. The site-scale studies can only talk about the intra-annual variation of carbon fluxes. Studying interannual variability in the carbon fluxes is not possible because the flux towers are only operational for one or two years. Furthermore, there are very few flux towers, and they are all concentrated in northern India. Because climate and growing conditions vary considerably across the wheat growing regions, it is impossible to extend these studies to understand carbon fluxes at regional scale.

Process-based model are widely used as an alternative to observations for studying carbon dynamics (Sándor et al., 2020). These models explicitly characterize known or hypothesized cause-effect links between physiological processes and driving forces in the environment (Chuine and Régnière, 2017). Process-based crop models, driven by atmospheric and other data as inputs, can simulate production, phenology, carbon and energy fluxes, and the interannual variability in the carbon budget of crops (Revill et al., 2019). The major advantage of using the process-based models is that they can be used to conduct numerical experiments to quantitatively evaluate the explicit effect of input parameters and external drivers on crop growth and fluxes (Jones et al., 2017). There are a couple of studies on carbon fluxes in terrestrial ecosystems of India (Banger et al., 2015; Gahlot et al., 2017) but they do not focus on agroecosystems.

This study used the Integrated Science Assessment Model (ISAM), a process-based land surface model with bio-geochemical and bio-geophysical components. ISAM was developed to assess the effect of variations in CO_2 concentration on agroecosystems (Jain and Yang, 2005; Song et al., 2013; Yang et al., 2009). ISAM was used for multiple regional and global-scale multimodel studies like the Global Carbon Budget (Le Quéré et al., 2018), the Trends in Net Land-Atmosphere Carbon Exchange (TRENDY) (Zhao et al., 2016), North American Carbon Program (NCAP) (Huntzinger

et al., 2012), Large-scale Biosphere-Atmosphere Experiment in Amazonia Data Model Intercomparison Project (LBA-DMIP) (De Gonçalves et al., 2013), and in comparing with forest FACE site observations (De Kauwe et al., 2013).

The broad goal of this study is to study carbon dynamics over spring wheat croplands of India and quantitatively estimate the role of different natural and anthropogenic drivers that govern carbon fluxes. The specific objectives of this paper are (i) to evaluate the capability of the ISAM model equipped with a spring wheat module to simulate carbon fluxes in spring wheat croplands by comparing them against field measurements; (ii) to study the spatiotemporal variation in carbon fluxes over spring wheat croplands of India over approximately four decades; and (iii) quantitatively estimate the effect of external drivers, including natural forcings like changing temperature and [CO_2] and agricultural management practices like nitrogen fertilization and water availability on carbon fluxes from spring wheat croplands of India.

To the best of our knowledge, there are no long-term regional-scale studies of carbon dynamics over Indian agroecosystems. As mentioned earlier, management practices can strongly affect crop growth and the interaction of crops with land and atmosphere through exchanges of water, energy, nutrients, and carbon. No studies have explored the impact of these management practices on the carbon fluxes in Indian agroecosystems. The current study would be the first to address these issues and hence play an important role in advancing our understanding of terrestrial carbon dynamics.

2 Methodology

2.1 Modeling Approach

Gahlot et al. (2020) had implemented a spring wheat module in ISAM and used it to simulate the phenology and production of spring wheat at the site scale for the spring wheat farm site at the Indian Agriculture Research Institute (IARI), Delhi, and regional scale for entire India. The experimental site at IARI was operational for three growing seasons- 2013-14, 2014-15, and 2015-16. Carbon fluxes were measured only during 2013-14 growing season and phenology data was measured during the latter two seasons. The ISAM was calibrated and validated using phenology observations from the 2014-2015 and 2015-2016 growing seasons (Gahlot et al., 2020). Taking this work forward, we used the same model to estimate the carbon fluxes in the spring wheat croplands of India. The modeling approach used in the study is as follows. First, the ISAM model

was run in site-scale mode to simulate the carbon fluxes at the IARI site driven by prescribed management data. The simulations were evaluated against field measurements from the IARI site for the 2013-2014 growing season. Next, ISAM was run in regional-scale mode to simulate carbon fluxes over wheat-growing regions of India spanning from 1901 to 2016. Finally, we conducted numerical experiments to simulate the impacts of environmental drivers and agricultural management practices on carbon fluxes.

2.2 Model Description

This study used the ISAM in the same configuration as Gahlot et al. (2020) to simulate India's spring wheat phenology and production. For brevity, here we only provide a brief description of the model and its configuration. More details are available in Gahlot et al (2020). ISAM has a module for simulating generic C3 crops driven by external forcings and associated land-atmosphere fluxes of carbon, nitrogen, water, and energy in the croplands (Song et al., 2013). The $ISAM_{C3\_crop}$ module has static phenology and prescribed LAI using observations from the Moderate Resolution Imaging Spectroradiometer (MODIS) aboard the Terra and Aqua satellites. The $ISAM_{C3\_crop}$ module used static root parametrization with fixed rooting depth and fixed root fraction in each soil layer. Gahlot et al. (2020) developed and implemented $ISAM_{dyn\_wheat}$ module that can simulate the phenology and fluxes in spring wheat croplands. $ISAM_{dyn\_wheat}$ differs from the static version in three schemes: dynamic phenology, carbon allotment, and vegetation structure growth. $ISAM_{dyn\_wheat}$ was equipped with dynamic planting date criteria and heat stress modules to simulate the effects of environmental factors on all aspects of spring wheat phenology. Both modules can be run at the site and regional scales at 0.5° X 0.5° spatial and one-hour temporal resolutions.

ISAM simulates the processes through which external drivers can affect crop growth. For example, temperature influences maximum carboxylation rates, which regulates carbon assimilation (Song et al., 2013). The ISAM model can simulate nitrogen dynamics and the interactive effects of carbon-nitrogen cycles caused by climate change or increasing [CO2] (Yang et al., 2009b). Nitrogen fertilisation through deposition onto the soil serves as a nitrogen input to the ISAM nitrogen cycle (A. Jain et al., 2009). When water and mineral N are scarce, the carbon cycle and its assimilation suffer because of reduced carbon allocation to leaves and stems (Song et al., 2013).

Added water through irrigation reduces the water stress on crops in water-limited situations, thereby increasing carbohydrate production.

2.3 Site Data

Field observations on carbon fluxes are limited in India, and none are available in the public domain. We obtained field observations of carbon fluxes for the 2013-14 spring wheat growing season from the IARI, Delhi, experimental spring wheat farm (Bhatia et al., 2014: Kumar et al.,2021). The farm covering 650 square meters is located at 28^{o}40' N, 77^{o}12' E. The site has an EC flux tower that gave Gross Primary Production (GPP), Total Ecosystem Respiration (TER), and Net Ecosystem Production (NEP). The tower had enough area to ensure an upwind stretch of homogeneous vegetation, which was essential for measuring fluxes using the EC technique (Schmid, 1994). The spring wheat crop was planted on 16 December 2013 at the site. Nitrogen fertilizer at the rate of 120 kg N/ha was applied in three instalments of 60 kg N/ha, 30 kg N/ha, and 30 kg N/ha on the planting day and 25th and 67th days after sowing, respectively. The field was irrigated five times throughout the growing season to avert water stress.

2.4 Meteorological and management data

All ISAM simulations need data for both environmental and anthropogenic drivers. We used annual atmospheric [CO_2] data from Le Quéré et al. (2018) and climate data from Viovy (2018) for both site scale and country scale simulations. The temporal resolution of the climate data is 6-hourly, and we interpolated the climate data to hourly values. The planting date, nitrogen, and irrigation data used for the site scale runs are described in Section 2.2.

For the country scale runs, we used nitrogen fertilizer data developed by Gahlot et al. (2020) by combining data from Ren et al. (2018) and Mueller et al. (2012). Data of harvested wheat area in a gridded format is needed (1980-2016) for calculating fluxes at a country scale in units of TgC/yr. We used spring wheat harvested area data developed by Gahlot et al. (2020), combining harvested area from Monfreda et al. (2008) and MAFW (2017).

2.5 Experimental Design

2.5.1 Site scale simulations at the IARI site

The ISAM model was calibrated and validated by Gahlot et al. (2020) using the phenology observations from the 2014-2015 and 2015-2016 growing seasons. We designed the site scale carbon flux experiment to evaluate the capability of ISAM model to replicate the carbon fluxes from field observations for the growing season 2013-14. To simulate the carbon fluxes at a site scale, the ISAM model was spun up for the 2013-14 growing season using climate data from Viovy (2018), annual atmospheric [CO_2] data from Le Quéré et al. (2018), and airborne nitrogen deposition data (Dentener, 2006) until the soil parameters reached a steady state. Further details on the site scale spin-up are available in Gahlot et al. (2020).

We used both variants of the ISAM, the C3 generic crop module ($ISAM_{C3\_crop}$) and the dynamic spring wheat crop module ($ISAM_{dyn\_wheat}$) developed by Gahlot et al. (2020), to simulate crop phenology and carbon fluxes for the 2013-14 growing season. For these simulations, we used the planting date, irrigation, and nitrogen fertilization schedule applied at the IARI site (Section 2.2).

2.5.2 Country-wide simulations over wheat-growing regions of India

The country-wide simulations were designed to understand the spatial variation of carbon fluxes across India's wheat growing regions by utilising the $ISAM_{dyn\_wheat}$ module. To simulate the carbon fluxes at a regional scale, ISAM was spun up for 1901 to maintain constant soil parameters such as temperature, moisture, and carbon and nitrogen pools. For the spin-up, we used the climate data from Viovy (2018) for the years 1901–1920, with airborne nitrogen deposition (Dentener 2006) and [CO2] (Le Quéré et al., 2018) held at levels of 1901 and neglecting nitrogen fertilizer and irrigation.

After a steady-state was observed in the soil parameters, we used ISAM to conduct regional-scale simulations over wheat-growing regions of India to understand the variability of carbon fluxes across diverse climate and management conditions (Ortiz *et al.* 2008) from 1901 to 2016. First, we conducted a control run (S_{CON}) driven by the annual [CO2] data, climate data, nitrogen fertilizer data, and full irrigation to meet crop water

needs. Irrigation is a crucial factor in spring wheat cultivation, where 93.6 % of the wheat area is equipped with irrigation (MOA 2016), and the Indo-Gangetic plains contribute a significant part to the total wheat area irrigated in India (Gahlot et al., 2020). Data on the exact volume of irrigation water was not available. Therefore, in the S_{CON} simulation, each grid cell was considered 100% irrigated so that there was no water stress on the crops (Gahlot et al. 2020).

Our analysis focused on the years 1980 to 2016. We analyzed country-scale model results as inter-decadal changes from the 1980s to the 2010s. We calculated decadal averages for various fluxes by dividing the total period into 1980s – 1980 to 1989, 1990s – 1990 to 1999, 2000s - 2000 to 2009, and 2010s - 2010 to 2016.

2.5.3 Experiments to estimate the effect of external drivers on carbon fluxes.

Environmental drivers like temperature and [CO2] and agricultural management practices like applying nitrogen fertilizers and irrigation influence spring wheat growth and are likely to influence carbon fluxes. We conducted four additional experimental simulations to quantitatively estimate the effect of these forcings. The details of the experiments are given in Table 1. In the Control run (S_{CON}), the model was driven by inputs based on observations that vary over time. In the experimental simulations, value of an input driver was kept constant during the study period, while others were allowed to vary as in the S_{CON} simulation. For example, in S_{Temp}, the input data for [CO_2], nitrogen, and irrigation were identical to that in S_{CON}, except for temperature, for which we used the de-trended 1900 – 1930 climatology. In the S_{N_Fert} case, the [CO2], temperature and irrigation were identical to that in $S_{CON,}$ and nitrogen fertilization is absent. The S_{Water} case is like $S_{CON,}$ with the only difference that precipitation climatology was used, and no additional water was provided to the soil through irrigation. We calculated the effect of the individual driver as the difference between the S_{CON} run and the numerical experiments.

Table 1

Numerical experiments conducted to evaluate the effect of external drivers on carbon fluxes using ISAM dynamic wheat crop for 1901 – 2016.

Numerical Experiment	**Temperature**	**[CO_2]**	**Nitrogen Fertilization**	**Irrigation**
Control (S_{CON})	Six hourly CRU-NCEP	Yearly values from Global Carbon Project Budget 2017	Grid-cell specific fertilizer amount	Hourly values to ensure no water stress
S_{Temp}	Climatological daily temperature prepared from the period 1900-1930	Identical to S_{CON}	Identical to S_{CON}	Identical to S_{CON}
S_{CO2}	Identical to S_{CON}	Fixed at 1901 level	Identical to S_{CON}	Identical to S_{CON}
S_{N_Fert}	Identical to S_{CON}	Identical to S_{CON}	No fertilizer	Identical to S_{CON}
S_{Water}	Identical to S_{CON}	Identical to S_{CON}	Identical to S_{CON}	No irrigation + No precipitation change

3 Results

3.1 Evaluation of ISAM site-scale simulations

Site scale simulations were required to evaluate the performance of the dynamic spring wheat module ($ISAM_{dyn\_wheat}$) implemented in ISAM by Gahlot et al. (2020) in simulating carbon fluxes. Our results show that the spring wheat module can simulate the magnitude and seasonality of carbon fluxes in spring wheat croplands better than the generic crop growth module in ISAM ($ISAM_{C3\_crop}$). Figure 1 and Table 2 compare $ISAM_{dyn\_wheat}$ and $ISAM_{C3\_crop}$ against site observations for monthly average fluxes for the 2013-2014 growing season. Figure 1 shows that

the observed carbon fluxes started increasing from leaf emergence in mid-December 2013. The fluxes increased till they reach their peaks in March, after which they declined till the harvest in April.

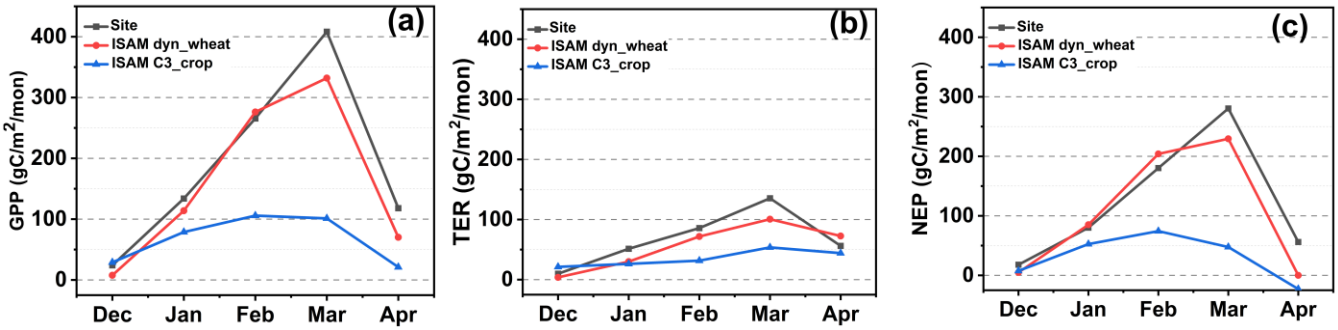

Figure 1: Comparison of observation and ISAM model fluxes (a) GPP, (b) TER, and (c) NEP.

The simulated fluxes followed the observed pattern. $ISAM_{dyn\_wheat}$ model run was in better agreement with site observations than the $ISAM_{C3\_crop}$ model. $ISAM_{dyn\_wheat}$ captured the seasonality and accumulated GPP, TER, and NEP for the growing season better than the $ISAM_{C3\_crop}$ model (Table 2). The $ISAM_{dyn\_wheat}$ peak coincided with the observations, whereas the fluxes simulated by the $ISAM_{C3\_crop}$ model peaked about a month earlier. The $ISAM_{dyn\_wheat}$ model in ISAM compares better with site measurements for plant biomass at harvest and maximum LAI than the $ISAM_{C3\_crop}$ model (Table 2).

Table 2

Various crop parameters of $ISAM_{dyn\_wheat}$ and $ISAM_{C3\_crop}$ against site measurements. We compared field observations at the IARI experimental wheat farm site and ISAM crop varieties, the dynamic crop and C3 generic crop, for the growing season of 2013-2014.

Variable	**Site**	**$ISAM_{dyn\_wheat}$**	**$ISAM_{C3}$**
Cumulative GPP (gC/m^2)	882	799.90	335.65
Cumulative TER (gC/m^2)	304	278.59	176.63
Cumulative NEP (gC/m^2)	576	523.30	159.02
TER/GPP	0.34	0.35	0.53

Plant Biomass at harvest (t/ha)	13.92	11.71	--
Correlation coefficient TER and GPP	0.86	0.81	0.24
Maximum LAI	4.6	6.0	1.10

Table 3 shows the Willmott index and RMSE for the two ISAM runs against the site observations. The Willmott index is a more sophisticated tool for evaluating the efficiency of land surface models compared to the usual statistical data comparison indices (Song et al., 2013; Willmott et al., 2012). The Willmott index (Eq. 1) ranges from -1 to 1, where -1 indicates no agreement while +1 indicates perfect agreement. The Wilmott index for GPP, TER, and NEP for the $ISAM_{dyn\_wheat}$ model are 0.85, 0.73, and 0.83, respectively. The corresponding values for the $ISAM_{C3\_crop}$ model are much lower at 0.47, 0.46, and 0.47, respectively. The higher index value for the dynamic crop suggested a better agreement of $ISAM_{dyn\_wheat}$ over $ISAM_{C3\_crop}$ with the site scale observations. Therefore, the $ISAM_{dyn\_wheat}$ model is more appropriate for representing spring wheat dynamics in the ISAM land model.

$$Willmot\ index = \begin{cases} 1 - \frac{\sum_{i=1}^{n}|Model_i - Obs_i|}{c * \sum_{i=1}^{n}|Obs_i - \overline{Obs}|}, if\ \sum_{i=1}^{n}|Model_i - Obs_i| \le c * \sum_{i=1}^{n}|Obs_i - \overline{Obs}| \\ \frac{c * \sum_{i=1}^{n}|Obs_i - \overline{Obs}|}{\sum_{i=1}^{n}|Model_i - Obs_i|} - 1, if\ \sum_{i=1}^{n}|Model_i - Obs_i| > c * \sum_{i=1}^{n}|Obs_i - \overline{Obs}| \end{cases} \quad (1)$$

$$\mathrm{RMSE} = \sqrt{\frac{\sum_{i=1}^{n}(\mathrm{Model_i} - \mathrm{Obs_i})^2}{n}} \quad (2)$$

where c = 2, n = number of observations, $Model_i$ represents the ISAM simulated carbon fluxes, and Obs_i represents the site scale observations.

Table 3

Willmott index and RMSE (gC/m^2/mon) of monthly carbon fluxes (GPP, NEP, and TER).

	Willmott index		**RMSE**	
	$ISAM_{dyn\_wheat}$	**$ISAM_{C3\_crop}$**	**$ISAM_{dyn\_wheat}$**	**$ISAM_{C3\_crop}$**
GPP	0.85	0.47	42.14	162.62
TER	0.73	0.46	20.82	45.90
NEP	0.83	0.47	36.05	120.44

3.2 Spatio-temporal variability of carbon fluxes from spring wheat agro-ecosystems in India

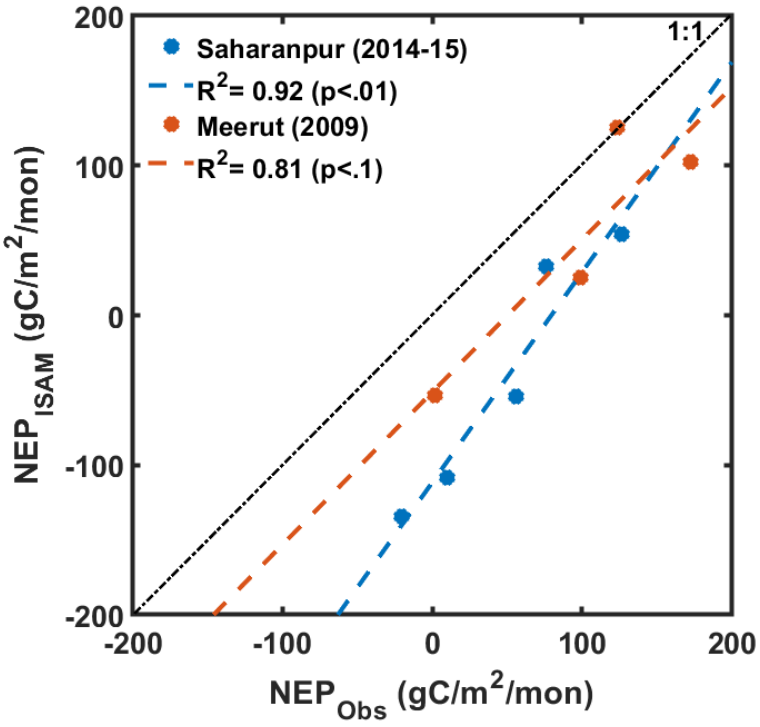

Figure 2: Comparison of the ISAM S_{CON} with the observations from Meerut (Patel et al., 2011) and Saharanpur (Patel et al., 2021).

The country-scale S_{CON} run described in Section 2.4b were designed to provide a quantitative understanding of the spatiotemporal variability of carbon fluxes across the wheat-growing regions of India. Before evaluating the regional scale ISAM runs, we decided to compare the simulated NEP from S_{CON} run with the carbon flux data from Patel et al. (2011, 2021). The monthly averaged carbon flux data was digitized from the figures. Patel et al. (2011) measured the carbon fluxes from Jan-Apr 2009 over a spring wheat farmland in Meerut in northern India. The measurements provided a diurnal variation of NEE during four growing stages- tillering, anthesis, post-anthesis, and at maturity. The diurnal data at a growing stage was averaged, and a value representing a monthly NEE was calculated and converted to NEP. Patel et al. (2021) provided daily NEE values at a spring wheat farmland in Saharanpur in northern India. The Patel et al. (2021) data was used to generate the monthly average fluxes for the growing season 2014-2015. The simulated NEP at the grid cells where Meerut and Saharanpur are located are extracted from the S_{CON} output. Figure 2 represents the comparison of simulated monthly average NEP (NEP_{ISAM}) and NEP_{OBS} measured

299 at Meerut (2009) and Saharanpur (2014-2015). The R^2 value for the stations is high, showing that
300 the ISAM simulated NEP captures the variation in observed NEP. The significance of the R^2 is
301 calculated using the two-tailed t-test, and the results reveal that R^2 is significant at $p<.01$ at
302 Saharanpur and $p<.1$ at Meerut. The mean absolute bias between observed and simulated NEP at
303 Saharanpur and Meerut are 90.61 $gC/m^2/mon$ and 50.227 $gC/m^2/mon$, respectively. The bias is
304 perhaps because we are comparing site-scale observations with simulated values that are averaged
305 over the 0.5^o x 0.5^o (~ 2500 km^2) grid cell area. Nonetheless, the high correlations with site
306 observations points to the robustness of the ISAM simulations.

307 Figure 3 shows the spatial maps of GPP, TER, and NEP for the growing season (December to
308 March). The fluxes for each month of the growing season were averaged over sixteen years (2000
309 - 2016) for that specific month. Because the climatic conditions across wheat-growing regions of
310 India are diverse, the wheat crops are sown on different dates, which was reflected in the ISAM
311 model using the dynamic planting day criteria. Spring wheat is planted in late October in Central
312 India and in early November in Eastern India. The planting dates for Northern and North-western
313 regions are late November to early December. Consequently, there are regional variations in the
314 seasonal flux dynamics. The central and eastern parts of the wheat-growing region show the
315 maximum value of fluxes in January and February, respectively, while the northern and western
316 parts show the maxima in March. The spatial plots show very low values of GPP and NEP during
317 December because the crops are still in early growth. The croplands show very low values of NEP
318 during March in the central and eastern parts of wheat-growing regions. Even though the croplands
319 are not active, heterotrophic respiration leads to moderate values of TER in March for the eastern
320 and central parts of India.

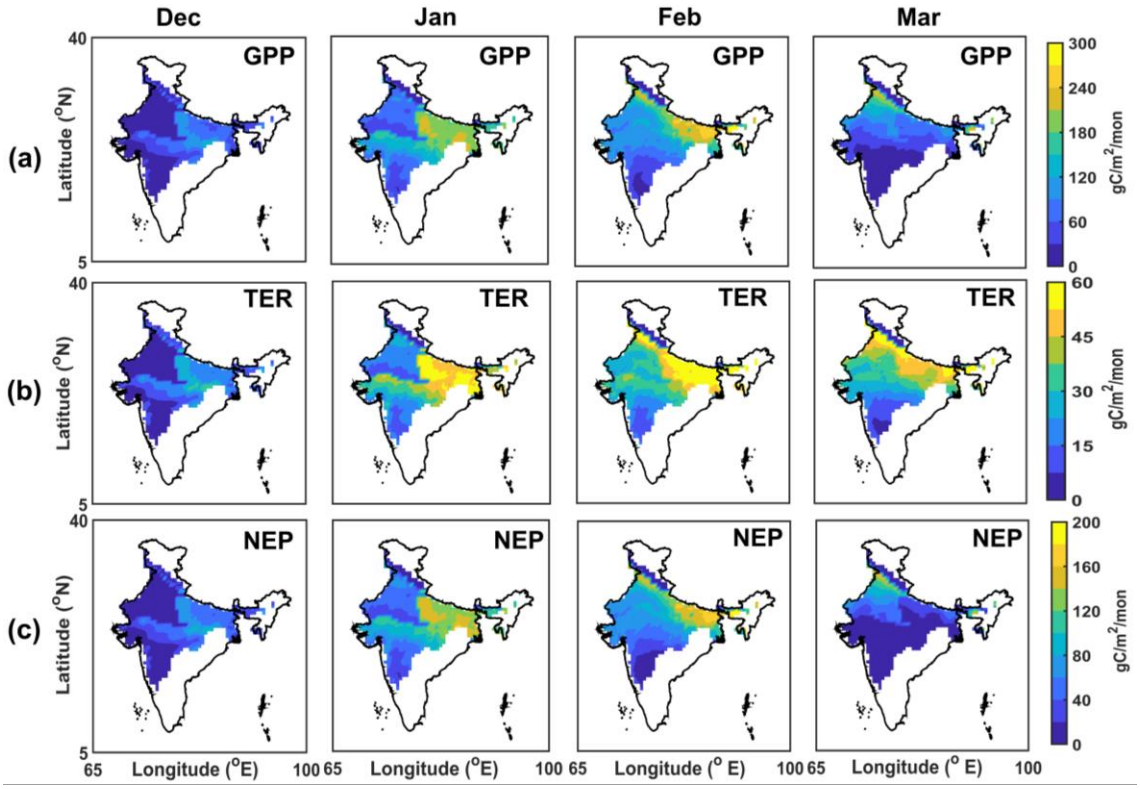

Figure 3: A spatial variation of (a) GPP, (b) TER, and (c) NEP over the wheat-growing regions of India averaged over the period 2000 to 2016.

Figure 4(a) depicts the temporal pattern of annual and decadal fluxes. From 1980 to 2016, the GPP, NEP, NPP, Ra, and Rh over the spring wheat croplands increased at 1.272, 0.945, 0.579, 0.328, and 0.366 TgC/yr^2, respectively. The trends represent the slope of the linear trend line, and the trends are significant at $p<.01$ calculated using a two-tailed test. Figure 4(b) shows the box-whisker plots. The box represents the 25-75 percentile of the data, and the whisker shows three times the interquartile range (3IQR). The data outside this 3IQR whisker is an extreme outlier. The median of all the fluxes showed a greater increase from the 1980s to 1990s compared to the 1990s to 2000s. The rise was again steep from the 2000s to the 2010s. Numerical experiments (Table 1) were conducted to explain the reasons for such behaviour. The results are described in the next section.

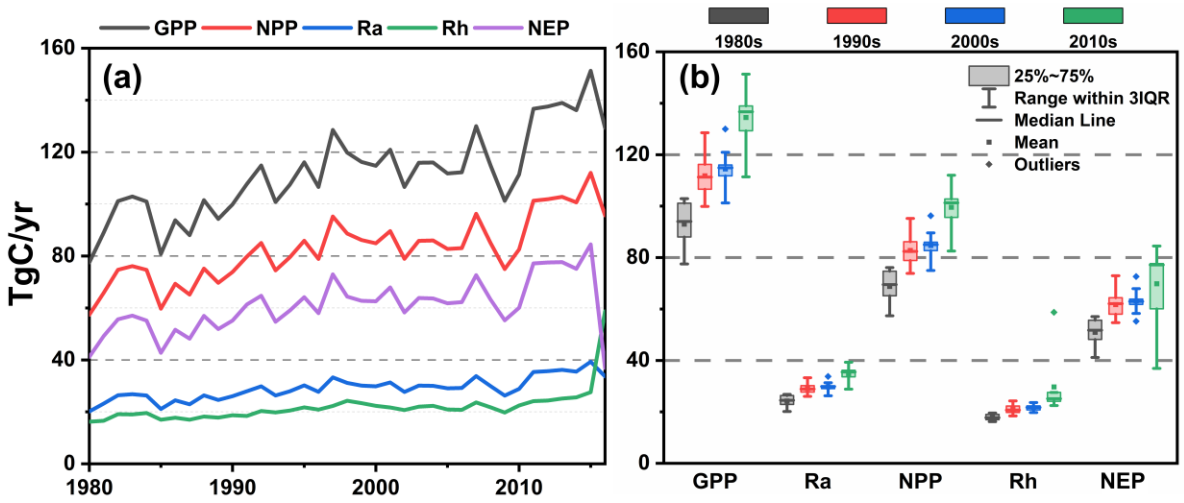

Figure 4: Carbon fluxes simulated by ISAM model. (a) The time series of fluxes from 1980 to 2016, (b) Decadal averages of fluxes.

3.3 Effects of external drivers on carbon fluxes

We investigated the impact of two climate drivers, changing temperature and [CO2], and two agricultural practices, nitrogen fertilizer and water availability due to irrigation, on carbon fluxes from spring wheat croplands. Figure 5 depicts the variation of these variables. Figure 5(a) shows the temperature anomaly between the S_{CON} and S_{Temp}. The temperatures are always warmer in S_{CON} compared to S_{Temp}. During the study period, the temperature anomaly increased at 0.038 ^{o}C/yr (Figure 5:(a)). [CO2] has also shown a consistent rise and increased at 1.743 ppm/yr (Figure 5:(b)). The nitrogen fertilizer added to the C3 crops increased at 1.86 kg/ha/yr over 36 years from 1980 to 2016 (Figure 5:(c)) (Hurtt *et al.* 2011). Figure 5(d) displays the anomaly in water present in the root zone during the growing season, estimated as the difference between S_{CON} and S_{Water}. Irrigation increases the amount of water available to crops during the growing season in the S_{CON} run. The S_{CON} run provides ~120 mm/season more water to the crop than the S_{Water} run, which is ~50% of the wheat crop water requirement during the growing season.

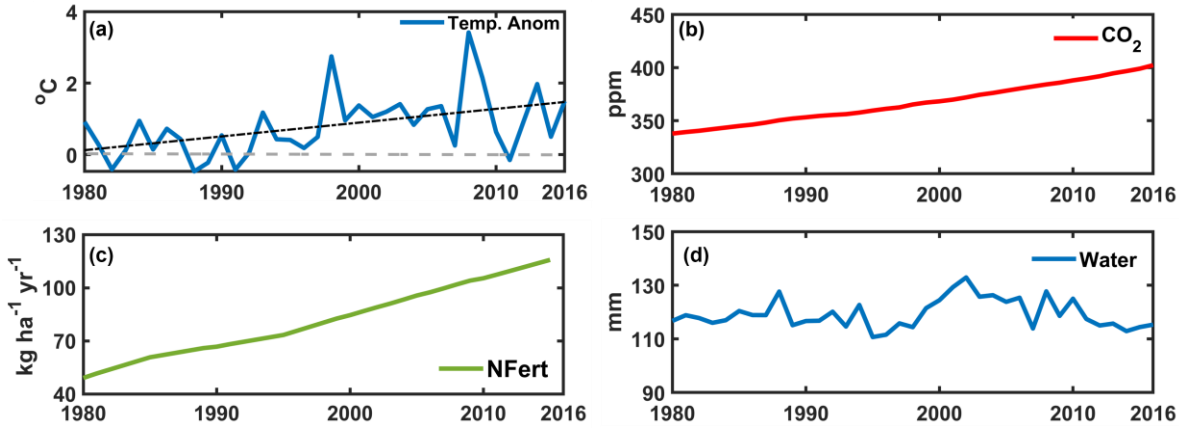

Figure 5: Time series of climate variables (a) Temperature anomaly, (b) Carbon Dioxide and management practice, (c) Nitrogen fertilization, and (d) Anomaly in water available in the root zone (S_{CON} - S_{Water}) during the growing season.

The effects of these factors are estimated by analyzing the difference in simulated carbon fluxes between the control and experimental simulation (Figure 6 and Table 4). Results show that the increase in temperature has a negative effect on all the fluxes. The temperature anomaly rose at 0.038 ^{o}C/yr, and yearly GPP decreased at 0.597 TgC/yr^2 during the study period. The temperature has varied less between the 1980s and 1990s; therefore, a slight difference in median GPP between these two decades is observed (Figure 6: (a)), although a higher spread in GPP is observed in the 1990s which is reflective of a few growing seasons with considerable temperature variation. The consistent higher temperatures during the 2000s and 2010s have caused a significant decrease in GPP. Since the temperatures considerably varied during the 2000s and 2010s, a large spread in simulated GPP can be observed. Similar trends in NPP and NEP can be observed with a decrease of 21.9 and 13.9 TgC/yr, respectively, per degree rise in temperature. Due to a temperature rise, the growing period and the crop phenology shortens (Koehler et al., 2013); hence a decrease in fluxes is observed. As the growth of the crop decreases, the TER and NEP also decreases.

Results showed that the increase in [CO_2] alone has led to a rise in annual GPP, NEP, Ra, and Rh at 0.805, 0.422, 0.201, and 0.175 TgC/yr^{2,} respectively (Table 4). During the study period, [CO_2] rose at 1.743 ppm/yr, causing an increase in GPP by 462 GgC per year for a unit ppm rise in [CO_2]. The GPP had a consistent rise each decade. A large spread in GPP was observed in the 1980s. The [CO_2] has consistently increased (Figure 5:(b)), but the temperature anomaly in the 1980s was below zero for a few growing seasons. Therefore, a significant variation in GPP and other fluxes

was observed (Figure 4:(a)) in this decade. Similarly, due to a higher CO_2 availability for the wheat crops, NPP, NEP, and TER have increased by 202, 100, and 173 GgC/yr per ppm rise in [CO2]. As the [CO_2] level increases in the environment, more carbon is available for crop uptake by photosynthesis (Saha et al., 2020).

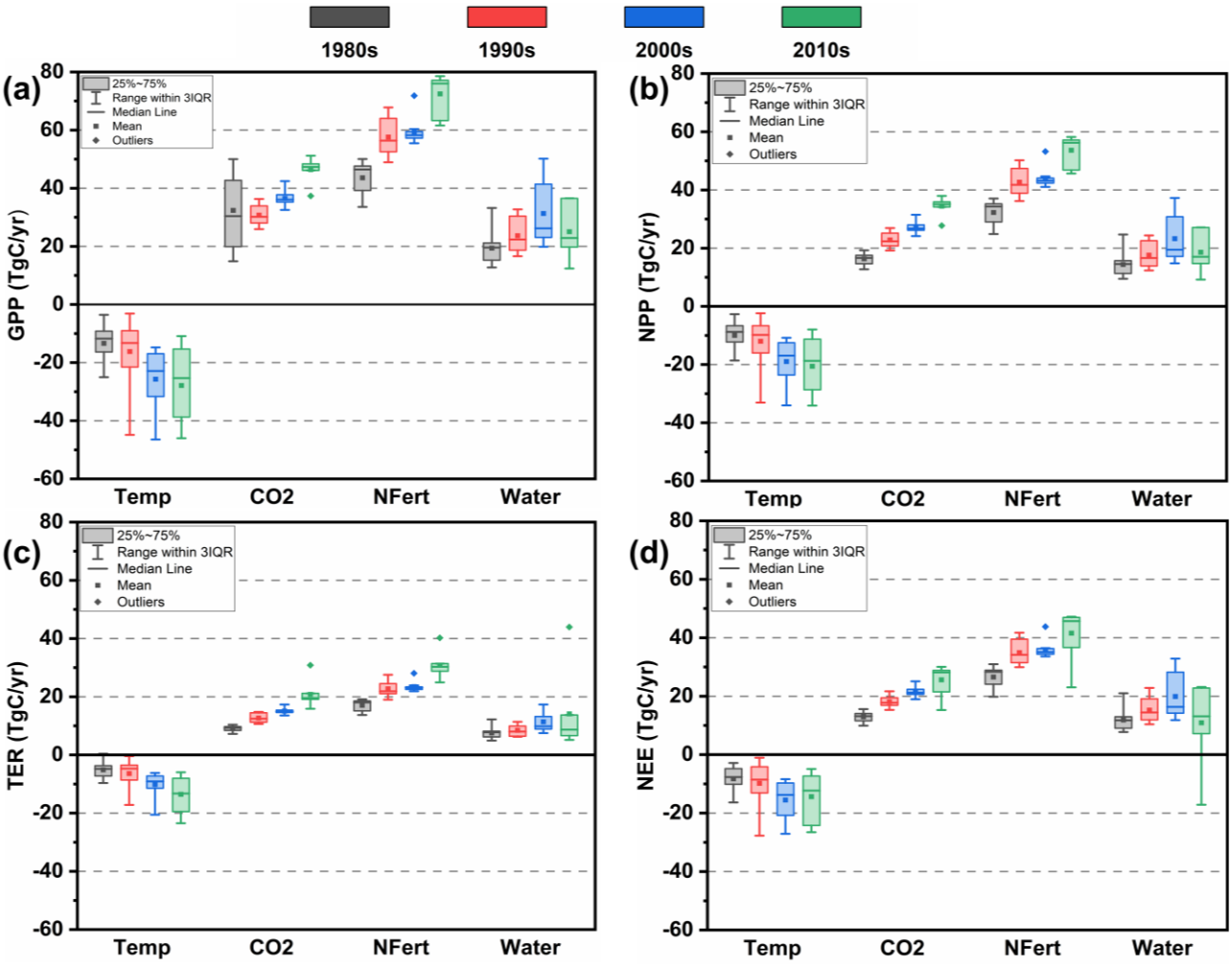

Figure 6: The Impact of various drivers (red- natural drivers: CO_2 and temperature, and blue- agricultural practices: irrigation and nitrogen fertilization) on wheat carbon fluxes. The impact of CO_2 is $S_{CON} - S_{CO2}$. Similarly, the impact of temperature is S_{CON}-S_{Temp}, nitrogen fertilization is S_{CON}-S_{N_Fert}, and irrigation is S_{CON}-S_{Water}.

Nitrogen fertilization has led to an increase in NEP, Ra, and Rh at 0.468, 0.231, and 0.197 TgC/yr^2, respectively. The impact of nitrogen fertilization on GPP at 0.897 TgC/yr^2 was the highest among all the factors. Nitrogen fertilization caused an increase in GPP by ~33 TgC on an annual basis.

Similarly, NEP increased by ~17 TgC/yr, Ra and Rh by ~8 and ~7 TgC/yr, respectively. Nitrogen fertilization is essential in India due to its tropical climate and multiple cropping systems (Gahlot et al., 2020). Studies have shown that nitrogen availability impacts the carbon uptake through the process of progressive Nitrogen limitation (A. Jain et al., 2009). Though the progressive nitrogen limitation is observed over longer timescales than the growing period of the crops, the decadal carbon flux simulations revealed some interesting results. Under excess [CO2] but nitrogen limited conditions, the crop growth does not show large difference and therefore the carbon uptake decreases (A. Jain et al., 2009; Luo et al., 2006). Under excess [CO2], if sufficient nitrogen is available then the carbon uptake by the ecosystem increases and therefore the maximum increase in fluxes was observed in the nitrogen fertilization case (Table 4). Nitrogen fertilization was consistent over the decades leading to a constant rise in GPP, but the variation in GPP in the 2000s was the least (Figure 6) caused by high temperatures during this decade (Figure 5). A similar pattern of low variation was observed in NEP, Ra, Rh and NEP during this period.

Table 4

The impact of each driver (TgC/yr^2) on various fluxes of the spring wheat crop in India. The values show the slope giving the linear trend of individual fluxes. *The trend has a significance level of $p < .01$.

Driver	**GPP**	**Ra**	**NPP**	**Rh**	**NEP**
Temperature	-0.597*	-0.159*	-0.438*	-0.185*	-0.278*
$[CO_2]$	0.805*	0.201*	0.597*	0.175*	0.422*
Nitrogen Fertilization	0.897*	0.231*	0.666*	0.197*	0.468*
Water	0.243	0.062	0.182	0.173	0.01

The impact of water added through irrigation led to an annual increase of ~9 TgC in GPP, ~6.5 TgC in NPP, ~2 TgC in Ra, and ~6 TgC in Rh. The reason for a small trend was that the fluxes have increased through the 1980s, 1990s, and 2000s, but declined in the 2010s. The reason for the decline was less water availability for the crops during this period, as shown in Figure 5(d). Therefore, the trends in these fluxes are not significant (Table 4). The higher GPP, NPP, and NEE in the 2000s compared to 1990s even though the temperatures were higher in 2000s suggested that

409 the adverse effects of high temperatures can be overcome if the crops are provided with enough
410 water.

411 **4 Discussions**

412 The ISAM simulations and especially the numerical experiments examining the impact of
413 temperature, [CO_2], nitrogen fertilization, and irrigation revealed some interesting features of the
414 spring wheat agroecosystem in India. All the fluxes have a similar pattern of high rise from 1980s
415 to 1990s, a small increase from 1990s to 2000s, and then a steep rise between 2000s and 2010s
416 (Figure 4:(b)). Although [CO_2] and Nitrogen fertilization increased at a constant rate throughout
417 the study period, the temperature and irrigation varied in an irregular manner. Higher temperatures
418 during the 2000s limited the rise in fluxes during this decade, and the lower water availability
419 during the 2010s caused a large spread in carbon fluxes in 2010s. The impact of [CO2] measured
420 through the difference between S_{CON} and S_{CO2} emphasised that with higher [CO2] the carbon taken
421 up for photosynthesis increases and the overall ecosystem exchange from the croplands was higher
422 than the limited [CO2] case. During the 2000s, a sudden dip in fluxes (Figure 4:(a)) was observed
423 that coincides with the higher temperature anomaly (Figure 5:(a)). However, the impact of added
424 water during this decade damped the negative effect of higher temperatures, which was evident
425 from the large spread seen in positive impact during this decade (Figure 6:(a-d)). Thus, the study
426 suggests that providing sufficient fertilizers and water through irrigation may be able to counteract
427 the adverse effects of high temperatures.

428 The simulated carbon fluxes are comparable to published values. The cumulative GPP and NEP
429 for the wheat-growing season observed at the Saharanpur site are 621 gC/m^2 and 192 gC/m^2 (Patel
430 et al., 2021). The GPP and NEP values simulated at the IARI site are 729.9 gC/m^2 and 523.3
431 gC/m^2. Although the GPP is comparable with Patel et al. (2021), NEP values simulated by ISAM
432 are not in the same range. The smaller NEP in Patel et al. (2021) is perhaps because the wheat crop
433 is grown immediately after sugarcane harvest with a fallow period of 30 days.

434 Additional work is required to overcome some of the limitations of this study. Perhaps the biggest
435 limitation of this study was in model evaluation. Ideally, multi-year data from numerous stations
436 across the study domain should be used for evaluation. However, carbon flux observations from
437 cropland in India were not available in the public domain. We used data from three agricultural

experimental sites in north India to evaluate the carbon fluxes simulated by ISAM. Even though the model evaluation was sub-optimal, this study is a step in the right direction because this is the first study to evaluate all terrestrial carbon fluxes simulated by a process-based model using site-scale observations.

Second, we estimated the effect of water availability on carbon fluxes by comparing the control simulation $S_{CON,}$ where the crops do not experience any water stress, with the S_{Water} simulation, where no irrigation is applied. The best way to understand the effect of irrigation would be to conduct simulations driven by actual irrigation data. For this purpose, we need a gridded irrigation time-series dataset. Unfortunately, such data does not exist (Gahlot et al., 2020) or is unrealistic in magnitude and timing (Mathur and AchutaRao, 2020).

Finally, our simulations were conducted with a land model driven by externally imposed forcings. In this approach, we ignored the feedback between the land surface and the atmosphere that can be important, especially for the natural drivers like [CO_2] and temperature. The next step moving ahead would be to use a coupled land-atmosphere model that includes the feedback between the terrestrial and atmospheric components of the carbon cycle.

5 Conclusions

We used the ISAM model equipped with a spring wheat module to study the carbon fluxes in spring wheat agroecosystems across the wheat-growing regions of India for the last four decades. The main conclusions from this study are as follows:

- The ISAM spring wheat module $ISAM_{dyn\_wheat}$ was able to simulate the temporal patterns of GPP, TER, and NEP at the site scale for the IARI experimental wheat farm. The $ISAM_{dyn\_wheat}$ model performed better compared to the generic $ISAM_{C3\_crop}$ module.
- Carbon fluxes in spring wheat agro-ecosystems varied widely across the country due to divergent climatic conditions and management practices, primarily due to difference in planting dates. While central and eastern parts of the spring wheat-growing regions showed high carbon fluxes during January, the northern parts exhibited their maximum carbon flux values during March.
- The effects of increasing [CO_2], nitrogen fertilization, and irrigation led to positive trends in carbon fluxes in the last four decades. Nitrogen fertilization had the strongest effects,

467 followed by [CO_2] and then water availability. Providing sufficient fertilizers and water
468 through irrigation can counteract the adverse effects of high temperatures.

469 Understanding the variability in terrestrial carbon fluxes is essential for understanding the carbon
470 cycle. Agroecosystems cover large parts of the terrestrial biosphere, with the spring wheat
471 agroecosystem being one of India's largest land use types. This paper is one of the first long-term
472 regional-scale studies to look at carbon dynamics in an Indian agroecosystem. The model
473 developed in this study, after appropriate calibration, can be used to study other agroecosystems
474 as well. Very importantly, it can serve as a tool to conduct numerical experiments to study future
475 scenarios and the effects of external drivers. Thus, this study is likely to play a crucial role in
476 advancing our understanding of terrestrial carbon dynamics and our ability to simulate its
477 behaviour.

478 **Acknowledgments**

479 This work was partially supported by the Indian Space Research Organization (ISRO) Biosphere
480 Geosphere Program (IGBP).

481 **Open Research**

482 The site-scale observations measured at IARI, New Delhi and the ISAM simulated carbon fluxes
483 data are available at: https://doi.org/10.5281/zenodo.5833742

484 **References**

485 Baldocchi, D., Chu, H., and Reichstein, M. (2018). Inter-annual variability of net and gross
486 ecosystem carbon fluxes: A review. *Agricultural and Forest Meteorology*, 249, 520–533.
487 https://doi.org/10.1016/J.AGRFORMET.2017.05.015
488 Banger, K., Tian, H., Tao, B., Ren, W., Pan, S., Dangal, S., and Yang, J. (2015). Terrestrial net
489 primary productivity in India during 1901–2010: Contributions from multiple
490 environmental changes. *Climatic Change*, 132(4), 575–588. https://doi.org/10.1007/s10584-
491 015-1448-5
492 Bhatia, A., Kumar, A., Jain, N., Sehgal, V. K., and Pathak, H. (2014). Seasonal Variation in Net
493 Carbon-dioxide Exchange in Rice and Wheat Fields of Northern India. Asiaflux Workshop:
494 Bridging Atmospheric Flux Monitoring to National and International Climate Change
495 Initiatives, Proceedings *Vol 1* 18-23, August 2014, International Rice Research Institute
496 (IRRI), Los Banos, Philippines.
497 Chakraborty, S., Tiwari, Y. K., Deb Burman, P. K., Baidya Roy, S., and Valsala, V. (2020).
498 Observations and Modeling of GHG Concentrations and Fluxes Over India in *Assessment of*
499 *Climate Change over the Indian Region*, 73-92, Eds. R. Krishnan, et al., Springer Nature,

Singapore.
Chen, C., Li, D., Zhiqiu, G., Tang, J., Guo, X., Wang, L., et al. (2015) Seasonal and interannual variations of carbon exchange over a rice-wheat rotation system on the North China Plain. *Adv Atmos Sci*, 32, 1365–1380. https://doi.org/10. 1007/s00376-015-4253-1
Chuine, I., and Régnière, J. (2017). Process-Based Models of Phenology for Plants and Animals. *Annual Review of Ecology, Evolution, and Systematics*, 48(1), 159–182. https://doi.org/10.1146/annurev-ecolsys-110316-022706
De Gonçalves, L. G. G., Borak, J. S., Costa, M. H., Saleska, S. R., Baker, I., Restrepo-Coupe, et al. (2013). Overview of the large-scale biosphere-atmosphere experiment in amazonia data model intercomparison project (LBA-DMIP). *Agricultural and Forest Meteorology*, 182–183, 111–127. https://doi.org/10.1016/j.agrformet.2013.04.030
De Kauwe, M. G., Medlyn, B. E., Zaehle, S., Walker, A. P., Dietze, M. C., Hickler, T., et al. (2013). Forest water use and water use efficiency at elevated CO2 : a model-data intercomparison at two contrasting temperate forest FACE sites. *Global Change Biology*, 19(6), 1759–1779. https://doi.org/10.1111/gcb.12164
Dentener, F. J. (2006). *Global Maps of Atmospheric Nitrogen Deposition, 1860, 1993, and 2050*. https://doi.org/10.3334/ORNLDAAC/830
FAOSTAT. (2019). Food and Agriculture Organization of the United Nations, Rome, Italy. Retrieved 14 May, 2021, from 2019 website: http://www.fao.org/faostat/en/#data/QC
Gahlot, S., Lin, T. S., Jain, A. K., Baidya Roy, S., Sehgal, V. K., and Dhakar, R. (2020). Impact of environmental changes and land management practices on wheat production in India. *Earth System Dynamics*, 11(3), 641–652. https://doi.org/10.5194/esd-11-641-2020
Gahlot, S., Shu, S., Jain, A. K., and Baidya Roy, S. (2017). Estimating Trends and Variation of Net Biome Productivity in India for 1980–2012 Using a Land Surface Model. *Geophysical Research Letters*, 44(22), 11,573-11,579. https://doi.org/10.1002/2017GL075777
Green, J. K., Seneviratne, S. I., Berg, A. M., Findell, K. L., Hagemann, S., Lawrence, D. M., et al. (2019) Large influence of soil moisture on long-term terrestrial carbon uptake. *Nature*, 565, 476–479. https://doi.org/10.1038/s41586-018-0848-x
Hatfield, J. L., and Prueger, J. H. (2015). Temperature extremes: Effect on plant growth and development. *Weather and Climate Extremes*, 10, 4–10. https://doi.org/10.1016/j.wace.2015.08.001
Huntzinger, D. N. N., Post, W. M. M., Wei, Y., Michalak, A. M. M., West, T. O. O., Jacobson, A. R. R., et al. (2012). North American Carbon Program (NACP) regional interim synthesis: Terrestrial biospheric model intercomparison. *Ecological Modelling*, 232, 144–157. https://doi.org/10.1016/j.ecolmodel.2012.02.004
Hurtt, G. C., Chini, L. P., Frolking, S., Betts, R. A., Feddema, J., Fischer, G., et al. (2011). Harmonization of land-use scenarios for the period 1500-2100: 600 years of global gridded annual land-use transitions, wood harvest, and resulting secondary lands. *Climatic Change*, 109(1), 117–161. https://doi.org/10.1007/S10584-011-0153-2/FIGURES/15
Jain, A. K., and Yang, X. (2005). Modeling the effects of two different land cover change data sets on the carbon stocks of plants and soils in concert with CO 2 and climate change. *Global Biogeochemical Cycles*, 19(2), 20. https://doi.org/10.1029/2004GB002349
Jain, A., Yang, X., Kheshgi, H., McGuire, A. D., Post, W., and Kicklighter, D. (2009). Nitrogen attenuation of terrestrial carbon cycle response to global environmental factors. *Global Biogeochemical Cycles*, 23(4). https://doi.org/10.1029/2009GB003519
Jha, C. S., Thumaty, K. C., Rodda, S. R., Sonakia, A., and Dadhwal, V. K. (2013). Analysis of

546 carbon dioxide, water vapour and energy fluxes over an Indian teak mixed deciduous forest
547 for winter and summer months using eddy covariance technique. *Journal of Earth System*
548 *Science*, 122(5), 1259–1268. https://doi.org/10.1007/s12040-013-0350-7
549 Jones, J. W., Antle, J. M., Basso, B., Boote, K. J., Conant, R. T., Foster, I., et al. (2017). Brief
550 history of agricultural systems modeling. *Agricultural Systems*, 155, 240–254.
551 https://doi.org/10.1016/j.agsy.2016.05.014
552 Koehler, A. K., Challinor, A. J., Hawkins, E., and Asseng, S. (2013). Influences of increasing
553 temperature on Indian wheat: quantifying limits to predictability. *Environmental Research*
554 *Letters*, 8(3), 034016. https://doi.org/10.1088/1748-9326/8/3/034016
555 Kumar, A., Bhatia, A., Sehgal, V.K., Tomer, R., Jain, N., and Pathak, H. (2021). Net Ecosystem
556 Exchange of Carbon Dioxide in Rice-Spring Wheat System of Northwestern Indo-Gangetic
557 Plains. *Land*, 10(7): 701. https://doi.org/10.3390/land10070701
558 Le Quéré, C., Andrew, R., Friedlingstein, P., Sitch, S., Hauck, J., Pongratz, J., et al. (2018).
559 Global Carbon Budget 2018. *Earth System Science Data*, 10(4), 2141–2194.
560 https://doi.org/10.5194/essd-10-2141-2018
561 Lin, T., Song, Y., Lawrence, P., Kheshgi, H. S., and Jain, A. K. (2021). Worldwide Maize and
562 Soybean Yield Response to Environmental and Management Factors Over the 20th and 21st
563 Centuries. *Journal of Geophysical Research: Biogeosciences*, 126(11).
564 https://doi.org/10.1029/2021JG006304
565 Lokupitiya, E., Denning, A. S., Schaefer, K., Ricciuto, D., Anderson, R., Arain, M. A., et al.
566 (2016). Carbon and energy fluxes in cropland ecosystems: a model-data comparison.
567 *Biogeochemistry*, *129*(1–2), 53–76. https://doi.org/10.1007/s10533-016-0219-3
568 Luo, Y., Hui, D., and Zhang, D. (2006). Elevated CO_2 stimulates net accumulations of carbon
569 and nitrogen in land ecosystems: a meta-analysis. *Ecology*, 87(1), 53–63.
570 https://doi.org/10.1890/04-1724
571 MAFW (2017) Directorate of Economics and Statistics, Ministry of Agriculture, Govt. of India.
572 *Agricultural Statistics at a Glance 2016*. Retrieved from
573 https://eands.dacnet.nic.in/PDF/Glance-2016.pdf
574 Mathur, R., and AchutaRao, K. (2020). A modelling exploration of the sensitivity of the India's
575 climate to irrigation. *Climate Dynamics*, 54(3–4), 1851–1872.
576 https://doi.org/10.1007/S00382-019-05090-8
577 MOA (2016) Status paper on wheat; Directorate of Wheat Development Ministry of Agriculture
578 Govt. of India 180 pp., available at: https://www.nfsm.gov.in/StatusPaper/Wheat2016.pdf
579 (last access: 14 May 2021)
580 Monfreda, C., Ramankutty, N., and Foley, J. A. (2008). Farming the planet: 2. Geographic
581 distribution of crop areas, yields, physiological types, and net primary production in the
582 year 2000. *Global Biogeochemical Cycles*, 22(1), 1022.
583 https://doi.org/10.1029/2007GB002947
584 Mueller, N. D., Gerber, J. S., Johnston, M., Ray, D. K., Ramankutty, N., and Foley, J. A. (2012).
585 Closing yield gaps through nutrient and water management. *Nature*, 490(7419), 254–257.
586 https://doi.org/10.1038/nature11420
587 Ortiz, R., Sayre, K. D., Govaerts, B., Gupta, R., Subbarao, G. V., Ban, T., et al. (2008). Climate
588 change: Can wheat beat the heat? *Agriculture, Ecosystems and Environment*, 126(1–2), 46–
589 58. https://doi.org/10.1016/j.agee.2008.01.019
590 Patel, N. R., Dadhwal, V. K. and Saha, S. K. Measurement and Scaling of Carbon Dioxide (CO_2)
591 Exchanges in Wheat Using Flux-Tower and Remote Sensing. *J Indian Soc Remote Sens* 39,

383 (2011). https://doi.org/10.1007/s12524-011-0107-1

Patel, N. R, Pokhariyal, S., Chauhan, P. and Dadhwal, V.K. (2021). Dynamics of CO2 fluxes and controlling environmental factors in sugarcane (C4)–wheat (C3) ecosystem of dry sub-humid region in India. *International Journal of Biometeorology*, 65, 1069–1084. https://doi.org/10.1007/s00484-021-02088-y

Pillai, N. D., Nandy, S., Patel, N. R., Srinet, R., Watham, T., and Chauhan, P. (2019). Integration of eddy covariance and process-based model for the intra-annual variability of carbon fluxes in an Indian tropical forest. *Biodiversity and Conservation*, 28(8–9), 2123–2141. https://doi.org/10.1007/s10531-019-01770-3

Ramadas, S., Kiran Kumar, T. M., and Pratap Singh, G. (2020). Wheat Production in India: Trends and Prospects. In *Recent Advances in Grain Crops Research*. https://doi.org/10.5772/intechopen.86341

Ren, X., Weitzel, M., O'Neill, B. C., Lawrence, P., Meiyappan, P., Levis, S., et al. (2018). Avoided economic impacts of climate change on agriculture: integrating a land surface model (CLM) with a global economic model (iPETS). *Climatic Change*, 146(3–4), 517–531. https://doi.org/10.1007/s10584-016-1791-1

Revill, A., Emmel, C., D'Odorico, P., Buchmann, N., Hörtnagl, L., and Eugster, W. (2019). Estimating cropland carbon fluxes: A process-based model evaluation at a Swiss crop-rotation site. *Field Crops Research*, 234(January), 95–106. https://doi.org/10.1016/j.fcr.2019.02.006

Saha, S., Das, B., Chatterjee, D., Sehgal, V. K., Chakraborty, D., and Pal, M. (2020). Crop growth responses towards elevated atmospheric CO2. In M. Hasanuzzaman (ed.), Plant Ecophysiology and Adaptation under Climate Change: Mechanisms and Perspectives I, pp 147 - 198, Springer Nature, Singapore. https://doi.org/10.1007/978-981-15-2156-0_6

Sándor, R., Ehrhardt, F., Grace, P., Recous, S., Smith, P., Snow, V., et al. (2020). Ensemble modelling of carbon fluxes in grasslands and croplands. *Field Crops Research*, 252(March). https://doi.org/10.1016/j.fcr.2020.107791

Schmid, H. P. (1994). Source areas for scalars and scalar fluxes. *Boundary-Layer Meteorology*, 67(3), 293–318. https://doi.org/10.1007/BF00713146

Song, Y., Jain, A. K., and McIsaac, G. F. (2013). Implementation of dynamic crop growth processes into a land surface model: Evaluation of energy, water and carbon fluxes under corn and soybean rotation. *Biogeosciences*, 10(12), 8039–8066. https://doi.org/10.5194/bg-10-8039-2013

Sonkar, G., Mall, R. K., Banerjee, T., Singh, N., Kumar, T. V. L., and Chand, R. (2019). Vulnerability of Indian wheat against rising temperature and aerosols. *Environmental Pollution*, 254, 112946. https://doi.org/10.1016/j.envpol.2019.07.114

Viovy, N. (2018). *CRUNCEP Version 7 - Atmospheric Forcing Data for the Community Land Model*. https://doi.org/10.5065/PZ8F-F017

Willmott, C. J., Robeson, S. M., and Matsuura, K. (2012). A refined index of model performance. *International Journal of Climatology*, *32*(13), 2088–2094. https://doi.org/10.1002/JOC.2419

Yang, X., Wittig, V., Jain, A. K., and Post, W. (2009). Integration of nitrogen cycle dynamics into the Integrated Science Assessment Model for the study of terrestrial ecosystem responses to global change. *Global Biogeochemical Cycles*, *23*(4), n/a-n/a. https://doi.org/10.1029/2009GB003474

Yoshimoto, M., Oue, H., and Kobayashi, K. (2005). Energy balance and water use efficiency of

rice canopies under free-air CO2 enrichment. *Agricultural and Forest Meteorology*, *133*(1–4), 226–246. https://doi.org/10.1016/j.agrformet.2005.09.010

Zeng, J., Matsunaga, T., Tan, Z. H., Saigusa, N., Shirai, T., Tang, Y., et al. (2020). Global terrestrial carbon fluxes of 1999–2019 estimated by upscaling eddy covariance data with a random forest. *Scientific Data 2020 7:1*, 7(1), 1–11. https://doi.org/10.1038/s41597-020-00653-5

Zhao, F., Zeng, N., Asrar, G., Friedlingstein, P., Ito, A., Jain, A., et al. (2016). Role of CO2, climate and land use in regulating the seasonal amplitude increase of carbon fluxes in terrestrial ecosystems: A multimodel analysis. *Biogeosciences*, 13(17), 5121–5137. https://doi.org/10.5194/bg-13-5121-2016